

Article

Modulation of Rab GDP-Dissociation Inhibitor Trafficking and Expression by the Transmembrane Protein 59 (TMEM59)

Haifeng Wang^{1,2,*}  and Tieqiao Wen^{2,*}

¹ Kaifeng Key Laboratory of Food Composition and Quality Assessment, School of Environmental Engineering, Yellow River Conservancy Technical Institute, Kaifeng 475004, China

² Laboratory of Molecular Neural Biology, School of Life Sciences, Shanghai University, Shanghai 200444, China

* Correspondence: wanghaifeng@yrcti.edu.cn (H.W.); wtq@shu.edu.cn (T.W.)

Abstract: Transmembrane protein 59 (TMEM59) is a type I transmembrane protein. However, the characterization and functions of TMEM59 in cells are not clear. Our results showed that TMEM59 localizes to vesicular structures. Further co-localization studies illustrated that TMEM59 is mainly distributed in the lysosome and acidic vesicular. TMEM59 movement between the nucleus and cell membrane was observed in living cells expressing TMEM59–EGFP fusion proteins. In addition, cell surface transport of amyloid precursor protein (APP) was significantly inhibited by TMEM59 and increased APP levels in HEK296T cells. TMEM59 also significantly inhibits transport of Rab GDP dissociation inhibitor alpha (GDI1) and Rab GDP dissociation inhibitor beta (GDI2), and further increases expression of GDI1 and GDI2 proteins in the cytoplasm. However, TMEM59 does not affect protein expression and localization of BACE2. These results suggest that TMEM59 may be involved in the packaging of acidic vesicles, modulated transport, and processing of APP, GDI1, and GDI2.

Keywords: TMEM59; localization; protein; GDI1; GDI2



Citation: Wang, H.; Wen, T. Modulation of Rab GDP-Dissociation Inhibitor Trafficking and Expression by the Transmembrane Protein 59 (TMEM59). *Separations* **2022**, *9*, 341. <https://doi.org/10.3390/separations9110341>

Academic Editor: Jun Dang

Received: 25 September 2022

Accepted: 1 November 2022

Published: 3 November 2022

Publisher's Note: MDPI stays neutral with regard to jurisdictional claims in published maps and institutional affiliations.



Copyright: © 2022 by the authors. Licensee MDPI, Basel, Switzerland. This article is an open access article distributed under the terms and conditions of the Creative Commons Attribution (CC BY) license (<https://creativecommons.org/licenses/by/4.0/>).

1. Introduction

Transmembrane protein 59 (TMEM59), also known as DCF1 (dendritic cell factor 1), is a type I transmembrane protein. TMEM59 is widely expressed in different organelles, including the mitochondria, Golgi apparatus, endoplasmic reticulum, endosomes, and lysosomes. TMEM59 affects the expression and localization of MGST1 in the mitochondria [1]. Amyloid precursor protein (APP) is an integral membrane protein expressed in many tissues and concentrated in the synapses of neurons as a regulator of synapse formation, neural plasticity, and iron export [2–4]. A recent study found that TMEM59 is involved in the post-translational processing of amyloid- β protein precursors, supporting a role for epigenetic change in late-onset Alzheimer's disease (LOAD) pathology [5]. β -site APP cleaving enzyme 2 (BACE2), a homolog of BACE1, functions differently from BACE1 in APP processing. An in vitro study showed that BACE2 is degraded through the macrophagy-lysosome pathway, and lysosomal inhibition affects BACE2 processing of APP [6].

In addition, the TAT–TMEM59 fusion protein was efficiently transduced into glioblastoma U251 cells and had an antitumor effect [7]. TMEM59 encoded a 42 kDa protein and could be successfully expressed both in *Escherichia coli* and neural stem cells (NSCs). Overexpression of the TMEM59 gene induced NSCs that were maintained in an undifferentiated status. After the TMEM59 gene was silenced, the NSC cells tended to differentiate into neurons and astrocytes [8]. Overexpression of TMEM59 significantly inhibited cell proliferation, migration, and invasion, and dramatically promoted apoptosis in the glioblastoma U251 cell line [9]. TMEM59 overexpression significantly increases neuropeptide Y expression, revealing that TMEM59 plays a critical role in energy balance [10]. A study of optogenetic behavior showed that *Natronomonas pharaonis* halorhodopsin (NpHR) suppressed the

behavior in *Drosophila* larvae and mice, whereas TMEM59 prevented this suppression [11]. A visual system study found that loss of TMEM59 in the primary visual cortex (V1) caused a sight deficit in mice, suggesting an unknown contact between the TMEM59 and GABA systems [12]. TMEM59 overexpression in a Parkinson's disease (PD) *Drosophila* model significantly ameliorated impaired locomotor behavior in third instar larvae and normalized neuromuscular junction growth. TMEM59 could degrade α -synuclein both in vivo and in vitro, suggesting degradation of alpha-synuclein delays neurodegeneration and increases lifespan in *Drosophila* [13]. In addition, TMEM59, as a regulator of autophagy, interacting with ATG16L1 led to the promotion of a functional complex between LC3 and ATG16L1, and promotion of LC3 lipidation and subsequent activation of autophagy [14].

To date, the mechanisms of TMEM59 function remain unclear, although it has been assumed that they occur in the secretory or endosomal–lysosomal pathways. The present study found that TMEM59 was localized to acidic vesicles and bidirectionally transported between the Golgi apparatus and the cell membrane. Overexpression of TMEM59 can inhibit APP, GDI1, and GDI2 localization to the cell surface, suggesting TMEM59 may mediate protein transport through regulated maturation and shedding of proteins.

2. Materials and Methods

2.1. Cell Culture

U251 human glioma cells, human embryonic kidney (HEK) 293T cells, 4T1 mouse mammary tumor cells, and U87 human glioma cells were purchased from the Chinese Academy of Sciences (Shanghai, China). U251, HEK293T, and U87 cells were grown in high-glucose Dulbecco's Modified Eagle Medium (DMEM, Gibco, Shanghai, China) with 10% fetal bovine serum (FCS, Gibco). The 4T1 cells were cultivated in Roswell Park Memorial Institute-1640 (RPMI-1640, Gibco) medium with 10% FCS. Mouse neural stem cells (NSCs) line C17.2 (kindly provided by Dr. Evan Y. Snyder) were grown in high-glucose DMEM with 10% FCS and 5% horse serum (HS, Gibco). All the cells were cultured in a humidified atmosphere with 5% CO₂ at 37 °C.

2.2. RNA Extraction and cDNA Synthesis

Total RNA was extracted from cells using the RNAiso™ Plus kit according to the supplier's specifications. A spectrophotometer (Eppendorf, Hamburg, Germany) was used to determine the concentration of RNA at 260/280 nm. cDNA was synthesized using 5 µg of total RNA from cells, and the ReverTra Ace Reverse Transcription System was used for first-strand synthesis following the manufacturer's instructions; it was then stored at –80 °C until use.

2.3. cDNA Cloning and Plasmid Constructing

Full-length human TMEM59 (hTMEM59) cDNAs were amplified from the human brain cDNA library (BioDev) and cloned into pEGFP-N2, pcDNA3.1(–)myc/his A, and pDsRed-Express-N1 vectors. In addition, the full-length mouse TMEM59 (mTMEM59) was also PCR amplified from the mouse brain cDNA library and cloned into pEGFP-N2 and pcDNA3.1(–)myc/his A vectors. Human APP, BACE2, GDI1, and GDI2 were cloned into pEGFP-N2. PCR products digested with double enzymes were purified using the Axyprep™ PCR Cleanup kit (AxyGEN, Union City, CA, USA). Plasmids were verified by sequencing, and primers used in this study are listed in Table 1.

Table 1. Primer sequences of full-length genes used to construct plasmids.

| Gene Symbol | Sequence (5'–3') | Plasmid |
|-------------|---|---------|
| hTMEM59 | 5'-CGGAATTCATGGCGGCGCCGAAGGGGAG-3' | N2 |
| | 5'-CGGGATCCGTAATAATTCAGAATGAGCA-3' | |
| | 5'-GATCTCGAGACCATGGCGGCGCCGAAGGGGAG-3' | 3.1(–)A |
| | 5'-CAGGAATTCATAATTCAGAATGAGCAAG-3' | |
| mTMEM59 | 5'-CGGAATTCATGGCGGCGCCGAAGGGGAG-3' | N1 |
| | 5'-CGGGATCCAGTAAAATTCAGAATGAGCA-3' | |
| | 5'-GATCTCGAGACCATGGCGGCGCCAAAGGGGAAG-3' | N2 |
| | 5'-CAGGAATTCGATTTCTGAGTGAGCAAGGTTTC-3' | |
| APP | 5'-GATCTCGAGACCATGGCGGCGCCAAAGGGGAAG-3' | 3.1(–)A |
| | 5'-CAGGAATTCGATTTCTGAGTGAGCAAGGTTTC-3' | |
| BACE2 | 5'-GACAAAGCTTATGCTGCCCGTTTGG-3' | N2 |
| | 5'-GATCCCGGGTCTGCATCTGCTCAAAGAACT-3' | |
| GDI1 | 5'-GATCTCGAGATGGGCGCACTGGC-3' | N2 |
| | 5'-GTAGGATCCGTTCCAGCGATGTCTGACC-3' | |
| GDI2 | 5'-GATAAGCTTATGGACGAGGAATACGAT-3' | N2 |
| | 5'-GTAGGATCCGCTGCTCAGCTTCTCCAAAG-3' | |
| GDI2 | 5'-GATCTCGAGATGAATGAGGAGTACGAC-3' | N2 |
| | 5'-GTAGGATCCGGTCTTCCCCATAGATGTCA-3' | |

2.4. Transfection

U251, HEK293T, 4T1, U87, and C17.2 cells were transiently transfected with Lipofectamine 2000 reagent (Invitrogen) when grown to 60–70% confluence. Cells were exposed to the DNA/Lipofectamine 2000 complex for 4 h in serum-free medium. After 6 h of transfection, the cell medium was replaced by fresh DMEM medium with 10% FBS. Cells were transfected for 36 h, then harvested and resolved in TRIzol Reagent for RNA extraction and reverse transcription.

2.5. Subcellular Localization of TMEM59

Twenty-four hours after transfection of the vectors, cells were washed three times with phosphate-buffered saline (PBS), fixed with 4% paraformaldehyde for 30 min, followed by washing with PBS. Cell nuclei were stained with DAPI for 5 min at room temperature. Golgi Tracker Red, LysoTracker Red, and MitoTracker Green were purchased from Beyotime Biotechnology Company (Shanghai, China). Golgi Tracker Red or Lyso Tracker Red dyes were used for labeling the Golgi apparatus and acidic cell organelles, respectively. MitoTracker Green was used for labeling the mitochondria.

2.6. Live Cell Imaging of TMEM59

For the analysis of TMEM59 movement in live cells, fluorescence was observed at 48 h after transfection of plasmids with a Nikon Eclipse TE2000-U fluorescence microscope. Images were collected using a spot CCD digital camera.

2.7. Western Blotting

HEK293T cells were co-transfected with EGFP-APP, EGFP-BACE2, EGFP-GDI1, EGFP-GDI2, and pcDNA3.1 (–) myc/his A-TMEM59. Cells were harvested by cell scraper, washed with cold PBST, and incubated in lysis buffer according to the manufacturer’s instructions. Samples were mixed with protein loading buffer, boiled for 5 min, and separated into 12% SDS-PAGE gels followed by transblotting to cellulose nitrate membranes (Whatman, Maidstone, Kent, UK) for 1 h at 25 V. The membranes were blocked with 1% BSA in PBST at room temperature and subsequently incubated with either anti-GFP, anti-myc, or anti-actin (1:2000; Santa Cruz) for 2 h at room temperature. The membranes were rinsed, incubated with a secondary antibody marked far-infrared signal (1:12,000; LI-COR, Lincoln, NE, USA) for 1 h, and scanned by an Odyssey scanner (LI-COR).

3. Results

3.1. TMEM59 Localizes to Vesicular Structures

The hTMEM59-EGFP fusion protein expression plasmid was respectively transfected into U251, C17.2, 4T1, and U87 cells. The pEGFP-N2 plasmid was used as a negative control. The results demonstrated that hTMEM59 localizes to vesicular structures in the cytoplasm and the perinuclear region. No EGFP staining was found in the nucleus (Figure 1). Similar to hTMEM59, the mTMEM59L-EGFP fusion protein also localized to vesicular structures in the cytoplasm and to the perinuclear region in U251, C17.2, and U87 cells (Figure 2).

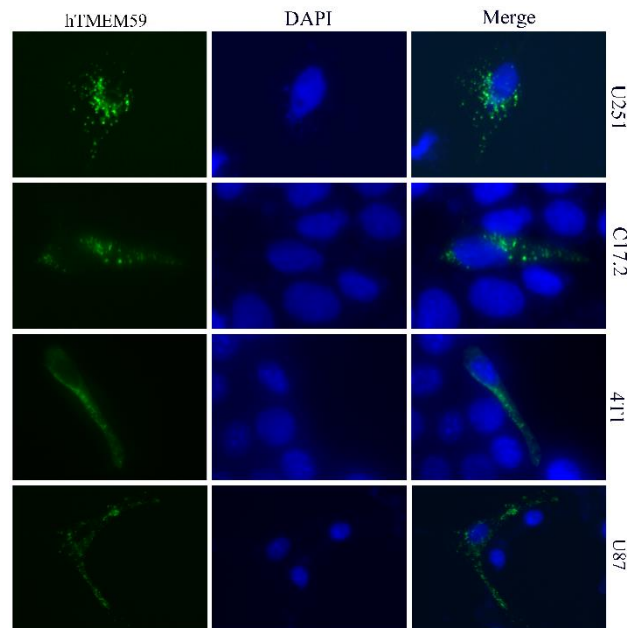


Figure 1. Intracellular localization of the human TMEM59 (hTMEM59) in different cells. U251, C17.2, 4T1, and U87 cells were transiently transfected with pEGFP-N2-hTMEM59, and 24 h later, the cells were observed under a fluorescence microscope and photographs were taken. The data showed that hTMEM59 is localized to vesicular structures in the cytoplasm and to the perinuclear region. DAPI represents cells and reflects the intracellular location of TMEM59.

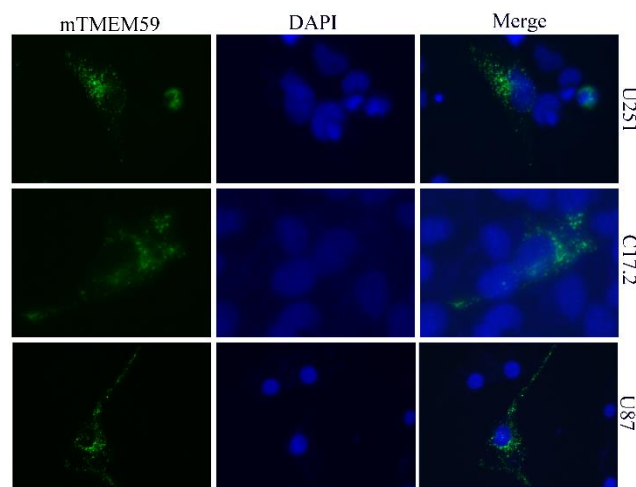


Figure 2. Intracellular localization of the mouse TMEM59 (mTMEM59) in different cells. U251, C17.2, and U87 cells were transiently transfected with pEGFP-N2-mTMEM59, and similar to hTMEM59L, mTMEM59 also localized to vesicular structures in the cytoplasm and to the perinuclear region. DAPI represents cells and reflects the intracellular location of TMEM59.

3.2. Movement of TMEM59 in the Cytoplasm

We used a fluorescence microscope to observe the localization of TMEM59-EGFP in the cell. The above results showed that TMEM59 is located in the perinuclear area, and some TMEM59 does not show static localization. Photos taken at an interval of 1 s are set to show that some TMEM59 moves in the cell. Dynamic movement of TMEM59, indicated by punctuated fluorescent signals in living cells, was seen in the cytoplasm when the TMEM59-EGFP fusion protein plasmid was transiently transfected into U251 cells (Figure 3).

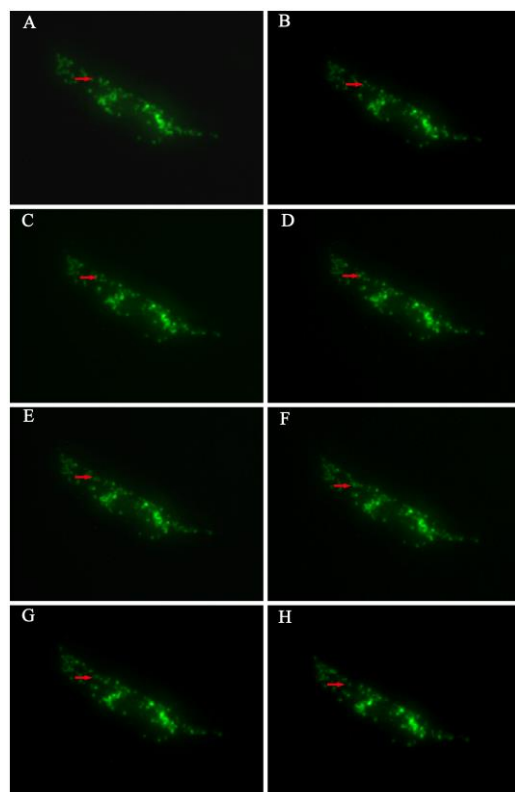


Figure 3. Movement of hTMEM59 in living C17.2 cells following interval photographs. (A–H) Punctuated fluorescent signals in the neurite and the cytoplasm, whereas the fluorescent signals also appeared dense and clustered in the perinuclear regions.

3.3. TMEM59 Localization in Lysosomes and Acidic Vesicles

TMEM59 subcellular localization was further assessed via Golgi Tracker Red and LysoTracker Red staining. The results demonstrated that TMEM59 and Golgi Tracker Red co-localize to the perinuclear regions in U251 cells. TMEM59 with LysoTracker Red was localized to lysosomes and acidic vesicular structures (Figure 4).

3.4. TMEM59 Increases APP Level but Has No Effect on BACE2

In control transfected HEK293T cells, EGFP-APP was observed in the cytoplasm and in the Golgi. In contrast, in cells co-transfected with TMEM59, APP fluorescence was found mainly in the Golgi and cytoplasmic staining was significantly decreased (Figure 5A). The expression level of APP was estimated by Western blotting, and the results showed that TMEM59 significantly increases the APP level in HEK293T cells (Figure 5B). Further studies indicated APP and TMEM59 colocalization to the Golgi (Figure 5C). However, it is interesting that BACE2 was not affected by TMEM59 (Figure 6).

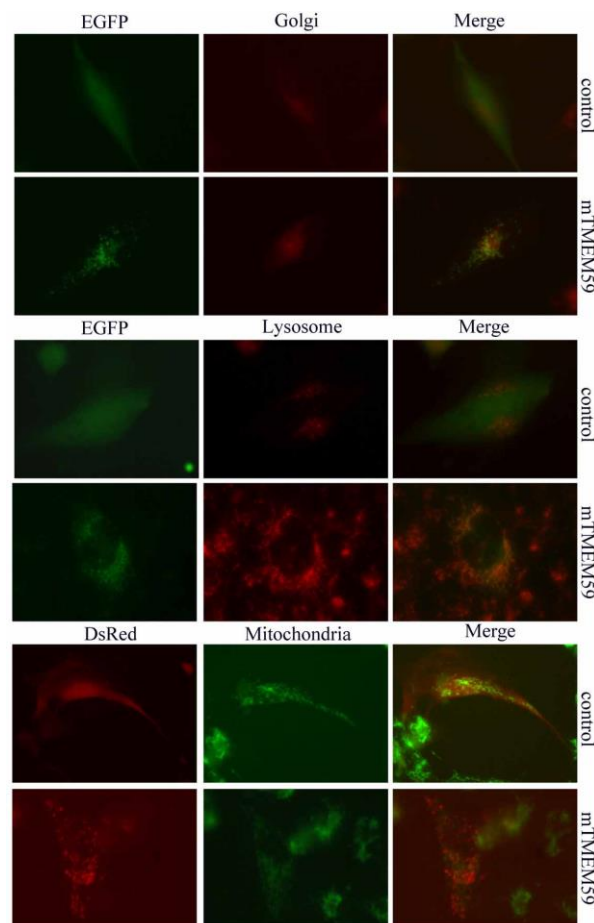


Figure 4. Subcellular localization of TMEM59. The TMEM59–EGFP fusion protein was transiently expressed in U251 cells. Golgi Tracker Red and LysoTracker Red staining are shown in parallel. TMEM59–DsRed was transiently expressed in U251 cells. MitoTracker Green is shown in parallel. All merged pictures are shown in the rightmost panels.

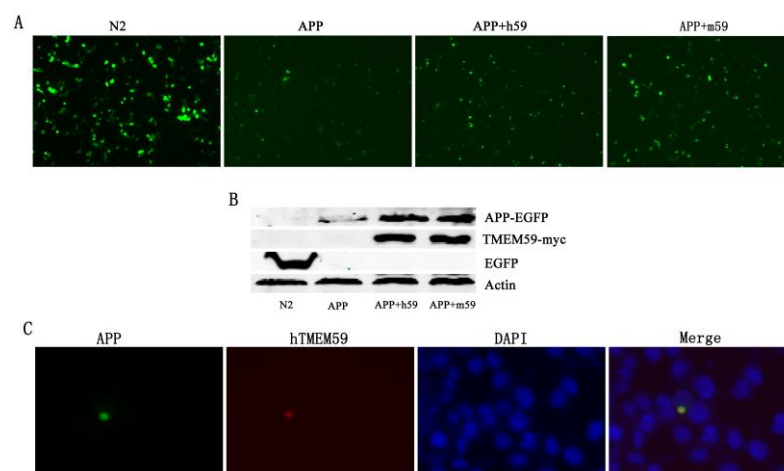


Figure 5. TMEM59 inhibits transport and increases the protein amount of APP. **(A)** Overexpression of TMEM59 leads to retention of APP in the cytoplasm. **(B)** TMEM59 increases the amount of APP protein in HEK293T cells. Western blotting showed that overexpression of TMEM59 increases the expression of APP. **(C)** TMEM59 and APP partially colocalize in the perinuclear region.

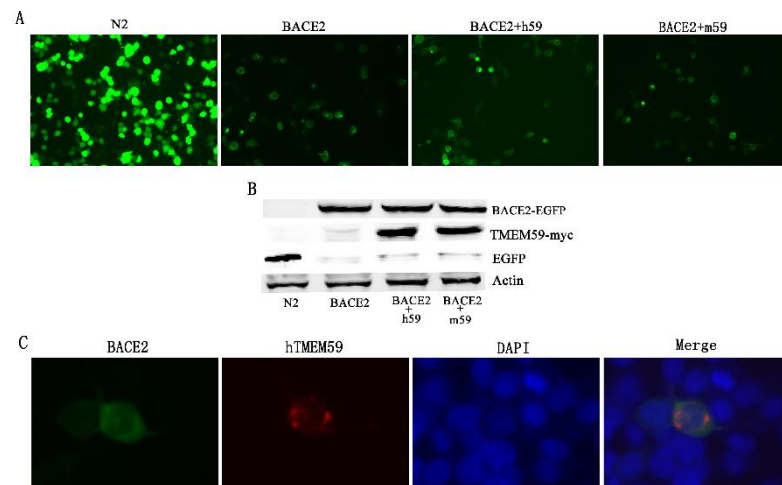


Figure 6. TMEM59 does not affect BACE2 protein expression. (A) TMEM59 did not change the localization of BACE2 in HEK293T cells. (B) The BACE2 protein level was not affected by TMEM59 in HEK293T cells. (C) TMEM59 and BACE2 showed no obvious colocalization in the cytoplasm.

3.5. Expression and Localization of GDI1 and GDI2 Were Changed by TMEM59

HEK293T cells were transiently co-transfected with GDI1/GDI2, and TMEM59 that showed fluorescence intensity was distinguished, as the cell tended to become round. GDI1 was detected by immunoblotting following TMEM59 being co-transfected into HEK293T cells. The results showed that TMEM59L induced GDI1 production increases in the cytoplasm. Similar to GDI1, GDI2 was also increased due to TMEM59 overexpression. Localization studies showed that the distribution of GDI1 and GDI2 tends to concentrate in the cytoplasm as a result of TMEM59 overexpression (Figures 7 and 8).

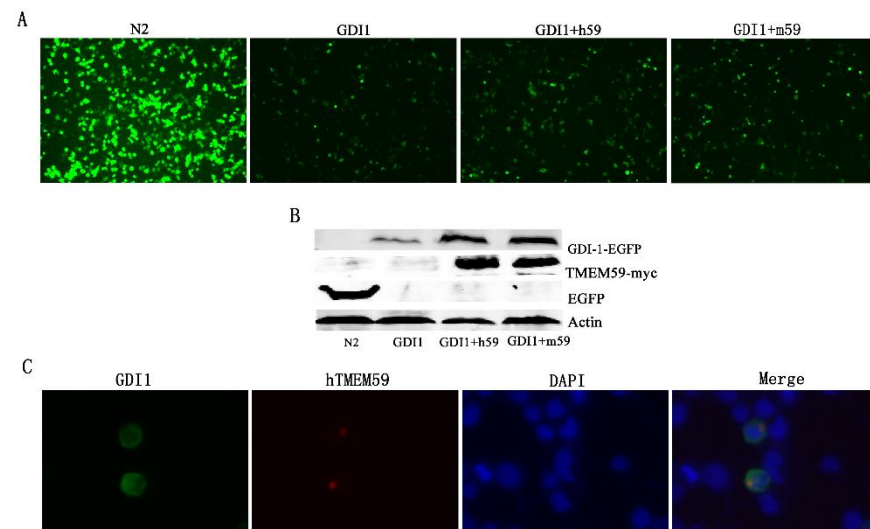


Figure 7. TMEM59 increases the protein amount of GDI1. (A) Overexpression of TMEM59 leads to retention of GDI1 in the cytoplasm. (B) TMEM59 increases the amount of GDI1 protein in HEK293T cells. Western blotting showed that overexpression of TMEM59 increases expression of GDI1. (C) TMEM59 and GDI1 show no obvious colocalization in the cytoplasm.

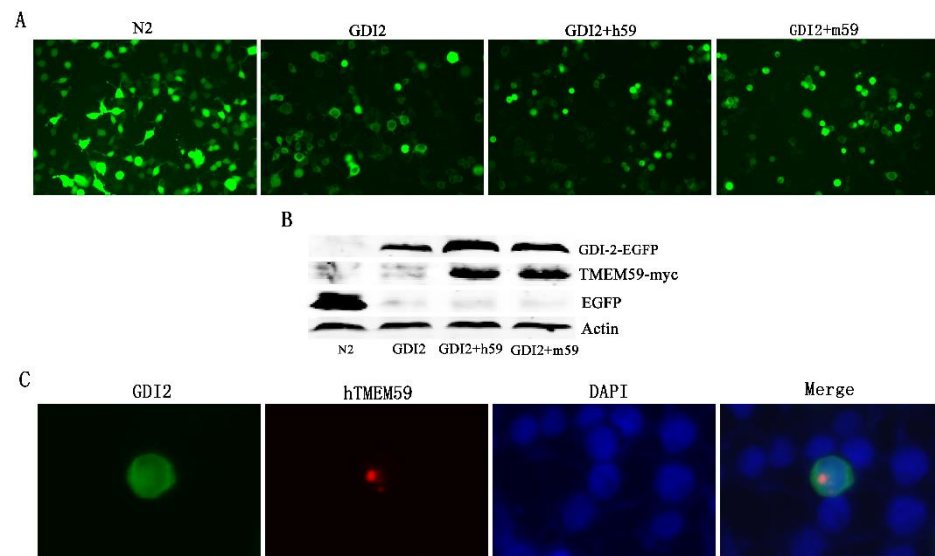


Figure 8. TMEM59 increases the protein amount of GDI2. (A) Overexpression of TMEM59 leads to retention of GDI2 in the cytoplasm. (B) TMEM59 increases the amount of GDI2 protein in HEK293T cells. Western blotting showed that overexpression of TMEM59 increases the expression of GDI2. (C) TMEM59 and GDI2 showed no obvious colocalization in the cytoplasm.

4. Discussion

TMEM59, a transmembrane protein that contains the WD40 domain-binding motif, disrupts its normal intracellular trafficking and its ability to engage ATG16L1 in response to bacterial infection [15]. Recent research showed that TMEM59 in the nervous system of mice induces social interaction deficiency and autism-like behavior, and it influences social interaction via the dopamine system [16]. TMEM59 knockout led to significantly perturbed expression of AMPA receptors (AMPA receptors) and induced morphological changes in astrocytes through the P38 signaling pathway [17]. MicroRNA-351 (miR-351) targets TMEM59 and negatively regulates TMEM59 expression in different cell types. Moreover, miR-351 overexpression led to morphological changes in the mouse NSC cell line C17.2 [18]. TMEM59 has been shown to potentiate Wnt signaling by promoting the formation of the Wnt receptor signalosomes. Transmembrane interactions between TMEM59 and the Wnt receptor Frizzled were found to drive receptor multimerization, leading to improved potency and efficacy of Wnt signaling [19]. A bioinformatics study demonstrated TMEM59 is an important factor contributing to Alzheimer’s disease (AD) from a compendium of expression profiles [20].

TMEM59 inhibits APP transport to the cell surface, and further shedding modulates the O-glycosylation and complex N-glycosylation steps occurring during the Golgi maturation of several proteins, such as APP, BACE1, SEAP, and PRNP. However, the precise function of TMEM59 is not known. Our study found TMEM59 localization in acidic vesicles and its bidirectional movement between Golgi and the cell membrane, and further experiments indicated increased protein expression and changed localization of APP through TMEM59 overexpression. To date, the mechanism of A β peptide production is still not very clear, although it has been assumed that A β formation may occur in the secretory or endosomal–lysosomal pathways. BACE2 is a close homolog of BACE1, a protease known to be an important enzyme involved in the cellular pathways, and BACE2 overexpression in cultured cells was found to lower net A β levels to a greater extent, but the physiological function and role of BACE2 in Alzheimer’s disease is unknown [21]. Our data showed TMEM59 does not affect the expression and localization of BACE2, which is different from BACE1. Vesicle shuttling is critical for many cellular and organismal processes, and GDP Dissociation Inhibitor (GDI) proteins contribute to vesicle shuttling by regulating the activity of Rab GTPases, controlling their cycling between the inactive cytosol and active

membrane-bound states. GDI are proteins that regulate the GDP–GTP exchange reaction of members of the Rab family, small GTP-binding proteins of the Ras superfamily that are involved in vesicular trafficking of molecules between cellular organelles [22–25]. GDI1 is expressed primarily in neural and sensory tissues. Mutations in GDI1 have been linked to X-linked nonspecific mental retardation [26]. Hsp90 co-localizes with Rab-GDI-1 and regulates agonist-induced amylase release in AR42J cells, and preferably interacts with Rab10 in insulin-stimulated GLUT4 translocation [27,28]. Our study found that overexpression of TMEM59 can inhibit expression and cell membrane localization of GDI1 and GDI2, suggesting that TMEM59 may, through mediated transport of GDI1 and GDI2, further affect maturation and shedding of APP.

In conclusion, our results provide a new perspective on the functionality of TMEM59. For the first time, we confirmed TMEM59 can increase protein expression of GDI1 and GDI2. However, unlike BACE1, TMEM59 does not affect protein expression and intracellular localization of BACE2. Given the intracellular localization of TMEM59 and its impact on the transport of vesicles involved in APP proteins, TMEM59 research should be focused on the field of signal guidance of protein localization. GDI1 and GDI2 are important regulatory proteins involved in intracellular vesicle trafficking, illustrating that protein localization is controlled through regulation of vesicle function by TMEM59. The results of this study suggest that TMEM59 may be an important contributor to protein-mediated transport and processing of proteins through the integrity of vesicle function.

Author Contributions: Editing, H.W.; methodology, H.W.; conceptualization and review, T.W. All authors have read and agreed to the published version of the manuscript.

Funding: This work was supported by the National Natural Science Foundation of China (No. 31070954) and the science and technology development plan of Kaifeng in 2020 (No. 2003048).

Institutional Review Board Statement: Not applicable.

Conflicts of Interest: The authors declare no conflict of interest.

References

1. Chen, Y.; Deng, Y.; Zhang, J.; Yang, L.; Xie, X.; Xu, T. GDI-1 preferably interacts with Rab10 in insulin-stimulated GLUT4 translocation. *Biochem. J.* **2009**, *422*, 229–235. [[CrossRef](#)] [[PubMed](#)]
2. Duce, J.A.; Tsatsanis, A.; Cater, M.A.; James, S.A.; Robb, E.; Wikke, K.; Leong, S.L.; Perez, K.; Johanssen, T.; Greenough, M.A. Iron-export ferroxidase activity of β -amyloid precursor protein is inhibited by zinc in Alzheimer's disease. *Cell* **2010**, *142*, 857. [[CrossRef](#)] [[PubMed](#)]
3. Priller, C.; Bauer, T.; Mitteregger, G.; Krebs, B.; Kretschmar, H.A.; Herms, J. Synapse formation and function is modulated by the amyloid precursor protein. *J. Neurosci.* **2006**, *26*, 7212–7221. [[CrossRef](#)] [[PubMed](#)]
4. Turner, P.R.; O'Connor, K.; Tate, W.P.; Abraham, W.C. Roles of amyloid precursor protein and its fragments in regulating neural activity, plasticity and memory. *Prog. Neurobiol.* **2003**, *70*, 1–32. [[CrossRef](#)]
5. Bakulski, K.M.; Dolinoy, D.C.; Sartor, M.A.; Paulson, H.L.; Konen, J.R.; Lieberman, A.P.; Albin, R.L.; Hu, H.; Rozek, L.S. Genome-wide DNA methylation differences between late-onset Alzheimer's disease and cognitively normal controls in human frontal cortex. *J. Alzheimer's Dis.* **2012**, *29*, 571–588. [[CrossRef](#)]
6. Xi, L.; Zhe, W.; Yili, W.; Jianping, W.; Weihong, S. BACE2 degradation mediated by the macroautophagy–lysosome pathway. *Eur. J. Neurosci.* **2013**, *37*, 1970–1977.
7. Wang, J.; Wang, Q.; Zhou, F.; Li, J.; Li, Q.; Zhou, H.; Li, S.; Ma, S.; Wen, T. The antitumor effect of TAT-DCF1 peptide in glioma cells. *Neuropeptides* **2018**, *71*, 21–31. [[CrossRef](#)]
8. Wang, L.; Wang, J.; Wu, Y.; Wu, J.; Pang, S.; Pan, R.; Wen, T. A novel function of dcf1 during the differentiation of neural stem cells in vitro. *Cell Mol. Neurobiol.* **2008**, *28*, 887–894. [[CrossRef](#)]
9. Xie, Y.; Li, Q.; Yang, Q.; Yang, M.; Zhang, Z.; Zhu, L.; Yan, H.; Feng, R.; Zhang, S.; Huang, C.; et al. Overexpression of DCF1 inhibits glioma through destruction of mitochondria and activation of apoptosis pathway. *Sci. Rep.* **2014**, *4*, 3702. [[CrossRef](#)]
10. Liu, Q.; Chen, Y.; Li, Q.; Wu, L.; Wen, T. Dcf1 regulates neuropeptide expression and maintains energy balance. *Neurosci. Lett.* **2017**, *650*, 1–7. [[CrossRef](#)]
11. Qiang, L.; Linhua, G.; Jian, N.; Yu, C.; Yanlu, C.; Zhili, H.; Xu, H.; Tieqiao, W. Dcf1 improves behavior deficit in drosophila and mice caused by optogenetic suppression. *J. Cell Biochem.* **2017**, *118*, 4210–4215.
12. Shi, J.; Li, Q.; Wen, T. Dendritic cell factor 1-knockout results in visual deficit through the GABA system in mouse primary visual cortex. *Neurosci. Bull.* **2018**, *34*, 465–475. [[CrossRef](#)] [[PubMed](#)]

13. Zhang, S.; Feng, R.; Li, Y.; Gan, L.; Zhou, F.; Meng, S.; Li, Q.; Wen, T. Degradation of alpha-synuclein by dendritic cell factor 1 delays neurodegeneration and extends lifespan in *Drosophila*. *Neurobiol. Aging* **2018**, *67*, 67–74. [[CrossRef](#)] [[PubMed](#)]
14. Romero, E.B.; Letek, M.; Fleischer, A.; Pallauf, K.; Ramón, C.; Pimentel-Muinos, F. TMEM59 defines a novel ATG16L1-binding motif that promotes local activation of LC3. *EMBO J.* **2013**, *32*, 566–582. [[CrossRef](#)] [[PubMed](#)]
15. Boada-Romero, E.; Serramito-Gómez, I.; Sacristán, M.P.; Boone, D.L.; Xavier, R.J.; Pimentel-Muinos, F.X. The T300A Crohn's disease risk polymorphism impairs function of the WD40 domain of ATG16L1. *Nat. Commun.* **2016**, *7*, 11821. [[CrossRef](#)] [[PubMed](#)]
16. Liu, Q.; Shi, J.; Lin, R.; Wen, T. Dopamine and dopamine receptor D1 associated with decreased social interaction. *Behav. Brain Res.* **2017**, *324*, 51–57. [[CrossRef](#)]
17. Wang, J.; Zhou, F.; Wang, D.; Li, J.; Lu, D.; Li, Q.; Zhou, H.; Li, W.; Wang, Q.; Wu, Y.; et al. Interaction of DCF1 with ATP1B1 induces impairment in astrocyte structural plasticity via the P38 signaling pathway. *Exp. Neurol.* **2018**, *302*, 214–229. [[CrossRef](#)]
18. Li, X.; Feng, R.; Huang, C.; Wang, H.; Wang, J.; Zhang, Z.; Yan, H.; Wen, T. MicroRNA-351 regulates TMEM 59 (DCF1) expression and mediates neural stem cell morphogenesis. *RNA Biol.* **2012**, *9*, 292–301. [[CrossRef](#)]
19. Gerlach, J.P.; Jordens, I.; Tauriello, D.V.F.; van 't Land-Kuper, I.; Bugter, J.M.; Noordstra, I.; van der Kooij, J.; Low, T.Y.; Pimentel-Muinos, F.X.; Xanthakis, D.; et al. TMEM59 potentiates Wnt signaling by promoting signalosome formation. *Proc. Natl. Acad. Sci. USA* **2018**, *115*, E3996–E4005. [[CrossRef](#)]
20. Zhang, L.; Ju, X.; Cheng, Y.; Guo, X.; Wen, T. Identifying Tmem59 related gene regulatory network of mouse neural stem cell from a compendium of expression profiles. *BMC Syst. Biol.* **2011**, *5*, 152. [[CrossRef](#)]
21. Abdul-Hay, S.O.; Sahara, T.; McBride, M.; Kang, D.; Leissring, M.A. Identification of BACE2 as an avid β -amyloid-degrading protease. *Mol. Neurodegener.* **2012**, *7*, 46. [[CrossRef](#)] [[PubMed](#)]
22. Bächner, D.; Sedlacek, Z.; Korn, B.; Hameister, H.; Poustka, A. Expression patterns of two human genes coding for different rab GDP-dissociation inhibitors (GDIs), extremely conserved proteins involved in cellular transport. *Hum. Mol. Genet.* **1995**, *4*, 701–708. [[CrossRef](#)] [[PubMed](#)]
23. Shisheva, A.; Buxton, J.; Czech, M. Differential intracellular localizations of GDP dissociation inhibitor isoforms. Insulin-dependent redistribution of GDP dissociation inhibitor-2 in 3T3-L1 adipocytes. *J. Biol. Chem.* **1994**, *269*, 23865–23868. [[CrossRef](#)]
24. Shisheva, A.; Doxsey, S.J.; Buxton, J.M.; Czech, M.P. Pericentriolar targeting of GDP-dissociation inhibitor isoform 2. *Eur. J. Cell Biol.* **1995**, *68*, 143–158. [[PubMed](#)]
25. Sedlacek, Z.; Konecki, D.S.; Korn, B.; Klauck, S.M.; Poustka, A. Evolutionary conservation and genomic organization of XAP-4, an Xq28 located gene coding for a human RAB GDP-dissociation inhibitor (GDI). *Mamm. Genome* **1994**, *5*, 633. [[CrossRef](#)] [[PubMed](#)]
26. Beranger, F.; Cadwallader, K.; Porfiri, E.; Powers, S.; Evans, T.; de Gunzburg, J.; Hancock, J. Determination of structural requirements for the interaction of Rab6 with RabGDI and Rab geranylgeranyltransferase. *J. Biol. Chem.* **1994**, *269*, 13637–13643. [[CrossRef](#)]
27. Chen, Y.; Feng, R.; Luo, G.; Guo, J.; Wang, Y.; Sun, Y.; Zheng, L.; Wen, T. DCF1 subcellular localization and its function in mitochondria. *Biochimie* **2018**, *144*, 50–55. [[CrossRef](#)]
28. Raffaniello, R.; Fedorova, D.; Ip, D.; Rafiq, S. Hsp90 Co-localizes with Rab-GDI-1 and regulates agonist-induced amylase release in AR42J cells. *Cell Physiol. Biochem.* **2009**, *24*, 369–378. [[CrossRef](#)]